⋆A Ludmila diz que a Nature physics não exige estrutura rígida do paper. Então fundi a seção Discussion com Conclusions.

⋆Movi a seção $\mu > 0$ ***do texto principal (e do Methods) para MS, e proponho tirar os cálculos detalhados de*** $\mu > 0$ ***do MS (parecem desnecessários neste paper) e a discussão dos 2-cycles do MS (já tem uma discussão no texto principal, e esses ciclos não são interessantes poque são os mesmos do LIF determinístico. Veja a seção "JUNK" no final.***

⋆Incorporei a maioria dos cortes da Ludmila na introdução, e cortei mais algumas palavras em outras seções. Ainda tem umas coisinhas para consertar e uns $\backslash$***obs para resolver.***

⋆Na minha última contagem, ainda tinha $\approx$***3100 palavras (sem contar abstract, métodos, bibliografia, fórmulas e figuras). Deve ter caído mais um pouco. Chegaremos lá...***

⋆Estou de volta. Espero terminar minha revisão em mais uma hora ou duas. –stolfi 2016-04-29 08:55:00

Phase transitions and self-organized criticality in networks of stochastic spiking neurons

Ludmila Brochini and Miguel Abadi

Departamento de Estatística, IME, Universidade de São Paulo, 05508-090, São Paulo, SP, Brazil

Ariadne de Andrade Costa and Jorge Stolfi

Instituto de Computação, Universidade de Campinas, 13083-852, Campinas, SP, Brazil

Antônio C. Roque and Osame Kinouchi

Departamento de Física, FFCLRP, Universidade de São Paulo,

14040-901, Ribeirão Preto, SP, Brazil

We report analytic and computational investigations of the behavior of neuronal networks with a general leaky stochastic neuron model, with neuron firing probability given by a function $\Phi(V)$ of the membrane potential V, rather than a sharp firing threshold. We found that the network can operate in various dynamic regimes (phases) depending on the model parameters, including the shape of the firing function Φ. In particular, for certain critical parameters we found a continuous phase transition to an absorbing stationary regime, in the directed percolation universality class, and also discontinuous phase transitions. In the continuous transition critical line we observe neuronal avalanches whose distributions of size and duration are given by power laws, as observed in real neuronal networks. We also propose the use of dynamical neuronal gains (a form of neuronal short-term plasticity), instead of dynamical synaptic strengths, as a more tractable mechanism to produce self-organized criticality (SOC) and neuronal avalanches.

Contents

I. INTRODUCTION

Integrate-and-fire (IF) neuron model were introduced the early 20th century [1] and have been extensively used in the simulation of neuronal networks [2–7]. In these models, the membrane potential $V(t)$ integrates synaptic and external currents up to a *firing threshold* value V_{T}. Then, a spike is generated and $V(t)$ drops to a *reset potential* V_{R}. The *leaky integrate-and-fire* (LIF) model extends the IF models with a leakage current, that causes the potential $V(t)$ to decay exponentially towards a *baseline potential* V_{B} in the absence of input signals [2, 4]. Despite their simplicity, these models have successfully emulated certain phenomenna observed in biological neuronal networks, such as firing avalanches [8–11] and multiple dynamical regimes [13, 14].

In the basic LIF models, the response of each neuron is deterministic. It has been claimed that a stochastic model may be more adequate for simulation purposes [15]. Some authors proposed to model those random influences by adding noise current inputs, both in continuous-time [2, 3, 13, 14] and discrete-time [16–19], resulting in the *leaky stochastic integrate-and-fire* (LSIF) model. In contrast, Galves and Löcherbach [20–22], and Larremore *et al.* [23] proposed to incorporate stochasticity into LIF models by assuming that the firing of a neuron is a random event, whose probability of occurrence in any time step is a *firing function* $\Phi(V)$ of membrane potential V. By subsuming all sources of randomness into a single function, this Galves-Löcherbach (GL) neuron model simplifies the analysis and simulation of neuronal networks.

Biological neural networks are known to exhibit *plasticity*: changes in neuronal parameters over time scales longer than the firing time scale, which are believed to be essential for higher functions like memory formation and learning [5, 24]. Short-term plasticity [25] has typically been incorporated in models by assuming that the strength of each synapse is lowered after each firing, and then gradually recovers towards a quiescent value [9, 10, 30, 31]. These changes have been observed to drive the parameters of the network towards critical values, which are believed to maximize its computational efficiency [8, 26–29]; a phenomenon called *self-organized criticality* (SOC).

In this article, we first study the dynamics of networks of GL neurons, by a simple mean-field approximation and by simulations of networks with thousands of elements. In the mean-field analysis, we replace the stochastic evolution of the network by a deterministic

evolution of a discrete probability distribution. We found both continuous and discontinuous phase transitions depending on characteristics of the firing function $\Phi(V)$. We found that, for certain firing functions and critical parameter values, the stimulated firing of a single neuron causes avalanches of firing events that are statistically similar to those observed in biological networks [8, 28].

Second, we present a new mechanism for short-term plasticity based on dynamical changes of a *gain* parameter associated to each neuron, instead of changing the individual synaptic strengths [9]. In our simulations, this new plasticity model proved sufficient to achieve self-organized criticality; but is much more efficient, since it has only one adaptive parameter per neuron, instead of one per synapse.

II. THE MODEL

We assume a network of N Galves-Löcherbach neurons that change state in parallel at certain *sampling times* with a uniform step Δ. Thus, the membrane potential of a neuron i is modeled by a sequence of real values $V_i[t]$, indexed by neuron number i (from 1 to N) and by the *discrete time* t, an integer that represents the sampling time $t\Delta$.

Each synapse transmits the signals from some *presynaptic* neuron j to some *postsynaptic* neuron i, and has a numerical attribute W_{ij}, the *synaptic strength*. We assume that $W_{ii} = 0$ for all i.

If some neuron j fires between discrete times t and $t+1$, its potential drops to V_R by time $t+1$. This event increments by W_{ij}/N the potential of every neuron i that does not fire in that interval. The potential of a non-firing neuron i may also integrate an *external input stimulus* $I_i[t]$, that can model neuronal or artificial signals from sources external to the network received between times t and $t+1$. Apart from these increments, the potential of a non-firing neuron decays exponentially by a factor $\mu \in [0,1]$, that models the effect of the leakage current.

We introduce the Boolean variable $X_i[t] \in \{0,1\}$ which denotes if neuron i fired between t and $t+1$. The potentials evolve as:

$$V_i[t+1] = \begin{cases} V_\mathsf{R} & \text{if } X_i[t] = 1, \\ \mu V_i[t] + I_i[t] + \dfrac{1}{N}\displaystyle\sum_{j=1}^{N} W_{ij} X_j[t] & \text{if } X_i[t] = 0. \end{cases} \tag{1}$$

Each $X_i[t]$ is assumed to be an independent random variable whose distribution depends on the potential $V_i[t]$. Namely, $X_i[t] = 1$ with probability $\Phi(V_i[t])$, for some specified *firing function* Φ [20, 21, 23].

We assume that Φ is sigmoidal: that is, monotonically increasing, with limiting values $\Phi(-\infty) = 0$ and $\Phi(+\infty) = 1$, and only one derivative maximum. We also assume that $\Phi(V)$ is zero up to some *threshold potential* V_T. If Φ is the shifted Heaviside step function Θ, namely $\Phi(V) = \Theta(V - V_\mathsf{T})$, we have a discrete time version of the deterministic LIF neuron. Any other choice for $\Phi(V)$ gives a stochastic neuron.

The network activity is measured by the fraction $\rho[t]$ of the neurons that fired between discrete times t and $t + 1$, namely:

$$\rho[t] = \frac{1}{N} \sum_{j=1}^{N} X_j[t] \,, \tag{2}$$

The fraction $\rho[t]$ can be computed from the distribution $P[t]$ of potentials at discrete time t:

$$\rho[t] = \int_0^\infty \Phi(V) P[t](V) \, dV \,, \tag{3}$$

where $P[t](V)\, dV$ is the fraction of neurons with potential in the range $[V, V + dV]$ at discrete time t. The neurons that fire between t and $t + 1$ have their potential reset to zero. They contribute to the distribution $P[t + 1]$ a Dirac impulse at potential $V = V_\mathsf{R}$, with amplitude (integral) $\rho[t]$ given by Eq. (3). In subsequent time steps, the potentials of all neurons will evolve in response to the firings of other neurons, according to Eq. (1). This process modifies $P[t]$ also for $V \neq V_\mathsf{R}$.

III. RESULTS

A. Analytic results for $\mu = 0$

We now develop a simple mean-field analysis of a network with no external inputs, in the limits $N \to \infty$ and $\mu \to 0$. The latter implies that, at time $t + 1$, the neuron "forgets" its previous potential $V_i[t]$ and integrates only the synaptic inputs $W_{ij} X_j$ received at time t. This scenario is interesting because it enables analytic solutions but exhibits all the kinds of phase transitions found with $\mu > 0$. In the Supplementary Material we give detailed calculations for this and other scenarios, including $\mu > 0$.

When $\mu = 0$, the potential distribution $P[t]$ consists of only two peaks at potentials $U_0[t] = V_\mathsf{R} = 0$ and $U_1[t] = W\rho[t-1]$, with fractions $\eta_0[t]$ and $\eta_1[t]$ that evolve by:

$$\eta_0[t+1] \;=\; \rho[t] \;=\; \Phi(V_\mathsf{R})\eta_0[t] + \Phi(W\eta_0[t])(1-\eta_0[t])\,, \tag{4}$$

with $\eta_1[t+1] = 1 - \eta_0[t+1]$. Furthermore, if $\Phi(V_\mathsf{R}) = 0$, Eq. (4) reduces to:

$$\eta_0[t+1] = \rho[t] = \Phi(W\eta_0[t])(1-\eta_0[t])\,. \tag{5}$$

In a stationary state, the variables in Eq. (5) become independent of time, and the equation simplifies to:

$$\rho = \Phi(W\rho)(1-\rho)\,, \tag{6}$$

with $\eta_0 = \rho$, $\eta_1 = 1-\rho$, $U_0 = 0$, and $U_1 = W\rho$. Note that $\Phi(W\rho)$ is at most 1, so any stationary solution must have $\rho \leq 1/2$.

a. The inactive regime: For any firing function with $V_\mathsf{T} \geq 0$, Eq. (6) has a solution $\rho = 0$, that corresponds to an *inactive* stationary state where $\rho[t] = 0$ for all t. If $V_\mathsf{T} > 0$, the solution is stable for any value of the other parameters. If V_T ¡ 0, this is not a stationary state. When $V_\mathsf{T} = 0$, its stability depends on the behavior of Φ at that potential, as discussed below.

b. The degenerate 2-cycle regimes: If the firing function is 1 above some finite saturation potential V_S, and W is greater than $W_\mathsf{B} = 2V_\mathsf{S}$, the condition for stationary state Eq. (6) reduces to $\rho = 1-\rho$, i.e. $\rho = 1/2$. This situation describes a degenerate stationary regime, in which half the neurons fire at each step.

When W is strictly greater than W_B, besides the stationary state with $\rho = 1/2$ there is an infinitude of regimes where the same potential distribution repeats with period 2 (*2-cycles*), and the activity $\rho[t]$ alternates between $1/2+\epsilon$ and $1/2-\epsilon$. In the (W,ρ) diagram, these periodic states are bounded by the lines:

$$\frac{V_\mathsf{S}}{W} \leq \rho \leq \frac{W - V_\mathsf{S}}{W}\,, \tag{7}$$

that bifurcate at the point $(W,\rho) = (W_\mathsf{B}, 1/2)$. See Fig. 1b. When $W > W_\mathsf{B}$, the stationary solution with $\rho = 1/2$ and the 2-cycles are marginally stable, since small perturbations will shift the network among these regimes. Note that these regimes are not a feature of the GL model: they also occur with the step firing function, i. e. in the deterministic LIF model.

B. The monomial firing functions

In this section we consider a specific class of firing functions with $V_\mathsf{T} = V_\mathsf{R} = 0$, the *saturating monomials*. The class is parametrized by a *degree* r and a *gain* $\gamma > 0$. In all these firing functions, $\Phi(V)$ is 0 when $V \leq V_\mathsf{T}$, and 1 when $V \geq V_\mathsf{S}$ where $V_\mathsf{S} = V_\mathsf{T} + 1/\gamma$. When $V_\mathsf{T} < V < V_\mathsf{S}$, we have:

$$\Phi(V) = [\gamma(V - V_\mathsf{T})]^r \,. \tag{8}$$

See Fig. 1a. Note that these functions can be seen as limiting cases of sigmoidal functions, and that we obtain the deterministic LIF model $\Phi(V) = \Theta(V - V_\mathsf{T})$ when $\gamma \to \infty$.

Here we consider only the case with $V_\mathsf{T} = V_\mathsf{R} = 0$. In the phase analyses that follow, the control parameters are W and γ, and $\rho(W, \gamma)$ is the order parameter.

a. The case $r = 1$ (continuous absorbing transition): For $W < W_\mathsf{B}$, when $r = 1$, Φ is the linear function $\Phi(V) = \gamma V$ for $0 < V < V_\mathsf{S} = 1/\gamma$. The stationary state condition Eq. (6) then becomes:

$$\gamma W \rho^2 + (1 - \gamma W)\rho = 0 \,. \tag{9}$$

The two solutions are $\rho = 0$ (the inactive state) and

$$\rho = \frac{W - W_\mathsf{C}}{W} \,. \tag{10}$$

Since we must have $0 < \rho \leq 1/2$, this solution is valid only for $W_\mathsf{C} < W \leq W_\mathsf{B}$ where $W_\mathsf{C} = 1/\gamma$. This solution describes a stationary state where $1 - \rho$ of the neurons are at potential $U_1 = W - W_\mathsf{C}$. The neurons that will fire in the next step are a fraction $\Phi(U_1)$ of those, which are again a fraction ρ of the total. In this case, the state $\rho = 0$ is unstable: any small perturbation of the potentials cause the network to converge to the active stationary state above. For $W < W_\mathsf{C}$, the solution $\rho = 0$) is stable and absorbing. In the W, ρ) phase diagram, the locus of stationary regimes defined by Eq. (10) bifurcates at $W = W_\mathsf{B}$ into the two bounds of Eq (7) that delimit the 2-cycles.

The condition $W = W_\mathsf{C}$ is a standard continuous absorbing state transition with a critical exponent $\alpha = 1$. In the (W, γ) diagram, the transition corresponds to a critical line $\gamma = \gamma_\mathsf{C}(W) = 1/W$, below the 2-cycle transition line $\gamma = \gamma_\mathsf{B}(W) = 2/W$. See Fig. 1c.

b. The case $r > 1$ (discontinuous transitions): For a monomial Φ with $r \neq 1$ and $W \leq W_\mathsf{B}$, the stationary state condition is:

$$(\gamma W)^r \rho^r - (\gamma W)^r \rho^{r-1} + 1 = 0 \,. \tag{11}$$

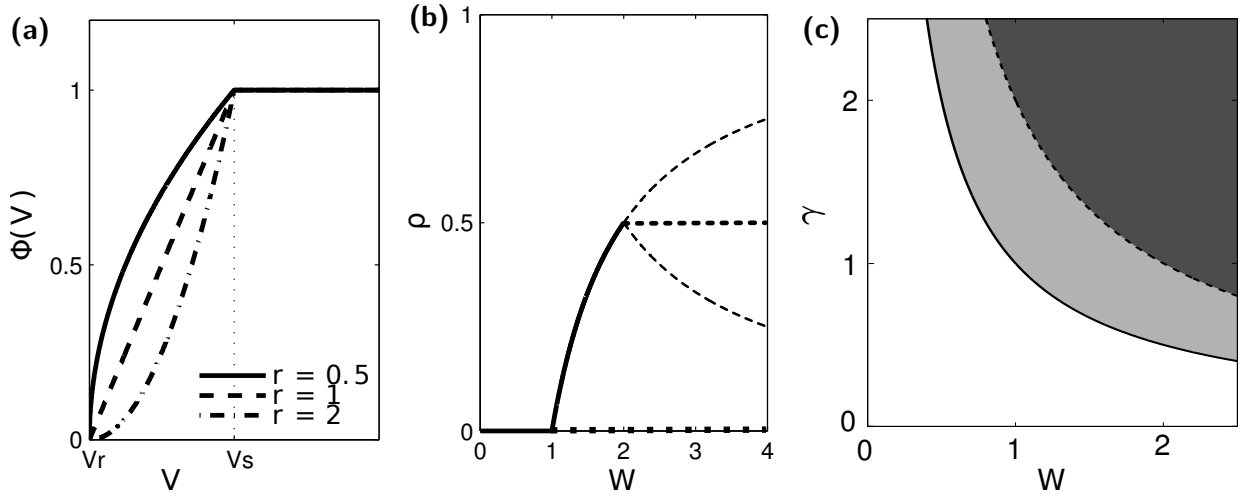

FIG. 1: (a) Examples of monomial firing functions $\Phi(V)$, with $V_{\mathsf{T}} = 0$, $\gamma = 1$ and $r = 1/2, 1$ and 2. (b) Fraction of firing neurons ρ as a function of the mean synaptic strength W for $r = 1$. The line bifurcates at $W_{\mathsf{B}} = 2/\gamma$ into two branches that bound the marginally stable 2-cycles. (c) The (W, γ) hase diagram for $r = 1$. Below the critical line $\gamma = \gamma_{\mathsf{C}}(W) = 1/W$ we have only the absorbing inactive state $\rho = 0$. Above the line $\gamma = \gamma_{\mathsf{B}}(W) = 2/W$ we have 2-cycles with marginal stability and, in between, a single stable stationary regime with $\rho = (W - W_{\mathsf{C}})/W < 1/2$.

This equation has a positive solution only when $1 \leq r \leq 2$ and $W_{\mathsf{C}}(r) < W \leq W_{\mathsf{B}}$, for a certain $W_{\mathsf{C}}(r) > 1/\gamma$. In this case, at $W = W_{\mathsf{C}}(r)$ there is a discontinuous (first-order) phase transition to a regime with a positive activity $\rho = \rho_{\mathsf{C}}(r) < 1/2$. See Fig. 2a. It turns out that $\rho_{\mathsf{C}}(r) \to 0$ as $r \to 1$, leading to the continuous phase transition in that limit. For $r = 2$ the only positive solution to Eq. (11) with $W \leq W_{\mathsf{B}}$ is $W = W_{\mathsf{C}}(2) = W_{\mathsf{B}}$ with value $\rho = \rho_{\mathsf{C}}(2) = 1/2$. For $r > 2$, the only active stationary state is the degenerate one, with $\rho = 1/2$ and $W \geq W_{\mathsf{B}}$.

c. The case $r < 1$ (small self-sustained activity): In the case of a monomial firing function with $V_{\mathsf{T}} = V_{\mathsf{R}} = 0$, $W < W_{\mathsf{B}}$, and $r < 1$, there is no positive solution to Eq. (11), and there is no phase transition, that is, $W_{\mathsf{C}}(r) = 0$ for any γ. In the $\rho \to 0$ limit, however, we get $W_{\mathsf{C}}(r) \to (1/\gamma)\rho^{(1-r)/r}$ with the solution $W_{\mathsf{C}}(r) = 0$ for any $r < 1$, a continuous phase transition at zero W. See Fig. 2b. Notice that we recover the correct value $W_{\mathsf{C}}(1) = 1/\gamma$ when $r \to 1$. Interestingly, this ceaseless activity $\rho > 0$ for any $W > 0$ seems to be similar to that found by Larremore *et al.* [23] with a $\mu = 0$ monomial model with inhibitory neurons.

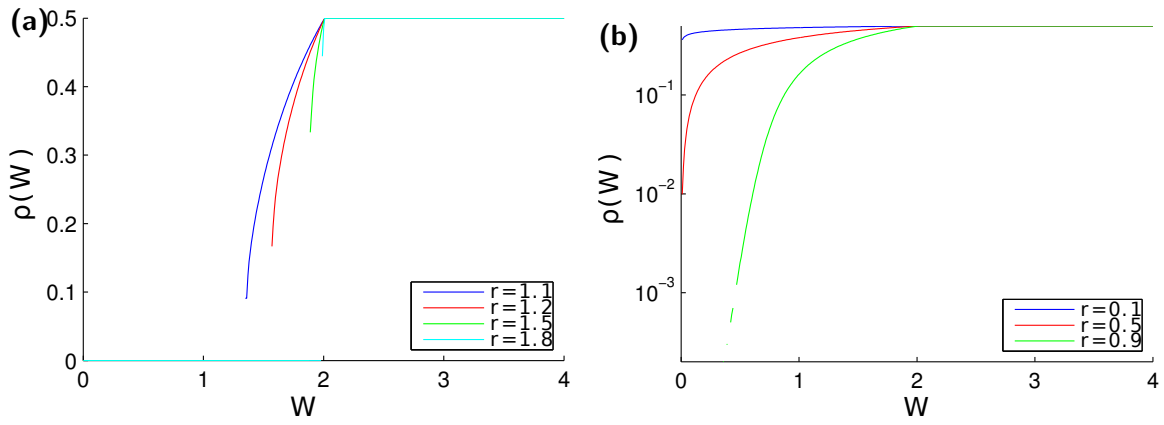

FIG. 2: (a) Discontinuous phase transitions for the monomial Φ with $\mu = 0$, $\gamma = 1$ with exponents $r = 1.1, 1.2, 1.5$ and 1.8. The discontinuity $\rho_{\mathsf{C}}(r)$ goes to zero for $r = 1$. (b) Ceaseless activity $\rho(W)$ for the monomial firing function with $\mu = 0$, $\gamma = 1$, with exponents $r = 0.1$, 0.5, and 0.9.

C. The rational firing functions

We have also analyzed the case when Φ is a *rational firing function*:

$$\Phi(V) = \frac{[\gamma(V - V_{\mathsf{T}})]^r}{1 + [\gamma(V - V_{\mathsf{T}})]^r}\,, \tag{12}$$

See Fig. 3a. Like the monomial functions, this class is parameterized by the exponent r and the gain γ. However, these functions only tend to 1 in the limit $V \to \infty$. Therefore, the degenerate stationary case with $\rho = 1/2$ and the 2-cycles do not appear, for any W and γ (i.e, $W_{\mathsf{B}} = +\infty$). Also, there are non-degenerate stationary states for all $r \geq 1$, whereas the monomial function admits only degenerate states with $r > 2$. Apart from these differences, the phase diagrams are determined by the exponent r in the same way as in the monomial case.

For the rational Φ with $V_{\mathsf{T}} = 0$, the stationary state condition is:

$$2(\gamma W)^r \rho^r - \frac{(\gamma W)^r}{\rho^{1-r}} + 1 = 0\,. \tag{13}$$

When $r = 1$, for any $W \geq W_{\mathsf{C}} = 1/\gamma$ there is a positive solution of equation Eq. (6) See Fig 3b. As in the monomial case, we find discontinuous (first-order) phase transitions when $r > 1$ (Fig. 4a) and ceaseless activity near $\rho = 0$ when $r < 1$ (Fig. 4b). The detailed analysis is given in the Supplementary material.

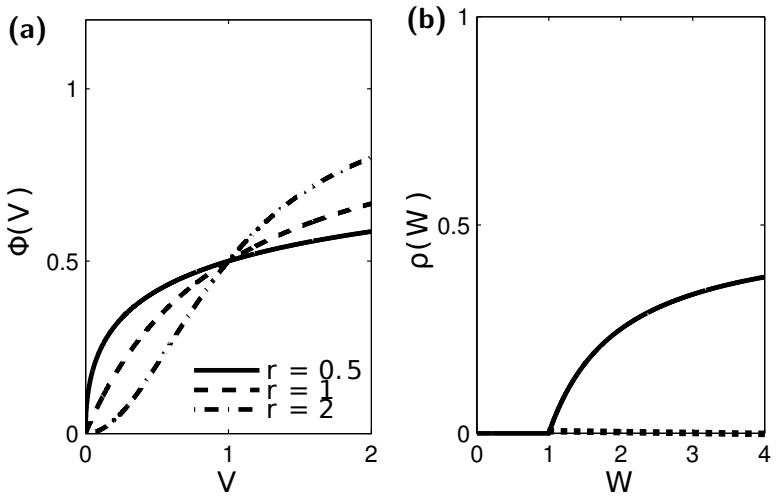

FIG. 3: (a) Examples of rational firing functions $\Phi(V)$: with $V_\mathsf{T} = 0$, $\gamma = 1$ and $r = 1/2, 1$ and 2 (from top to bottom). (b) Fraction of firing neurons ρ in a stationary regime as a function of W, for the rational firing function with $r = 1$.

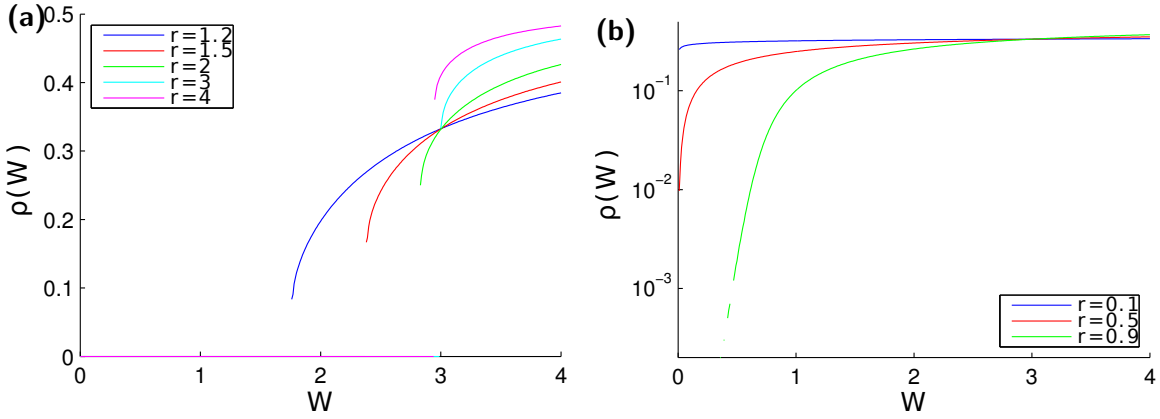

FIG. 4: (a) Discontinuous phase transitions for the rational firing function with $\mu = 0$ and $\gamma = 1$, for $r = 1.2, 1.5, 2.0, 3.0$ and 4.0. The discontinuity ρ_C goes to zero for $r = 1$. (b) Ceaseless activity $\rho(W)$ for the rational model with $\mu = 0$, $\gamma = 1$, with exponents $r = 0.1$, 0.5, and 0.9.

D. Neuronal Avalanches

Avalanche processes in neuronal networks have attracted significant interest, because of their possible connection to efficient information processing [8, 26, 28, 29]. Through numerical simulations, we also studied the critical point $W_\mathsf{C} = 1, \gamma_\mathsf{C} = 1, \mu = 0$ in search for neuronal avalanches [8, 28] (Fig 5a). Indeed, we observed a power law avalanche size distribution $P(S) \propto S^{-\beta}$ (Fig. 5b), with the mean-field exponent $\beta = 3/2$ [8, 10, 28, 30, 31].

We also used the complementary accumulated function $C(S) = \sum_{S=1}^{\infty} P(S)dS$ to perform data collapse, and scaling with N, obtaining the cutoff exponent $c_S = 1/2$ (Fig. 5c,d).

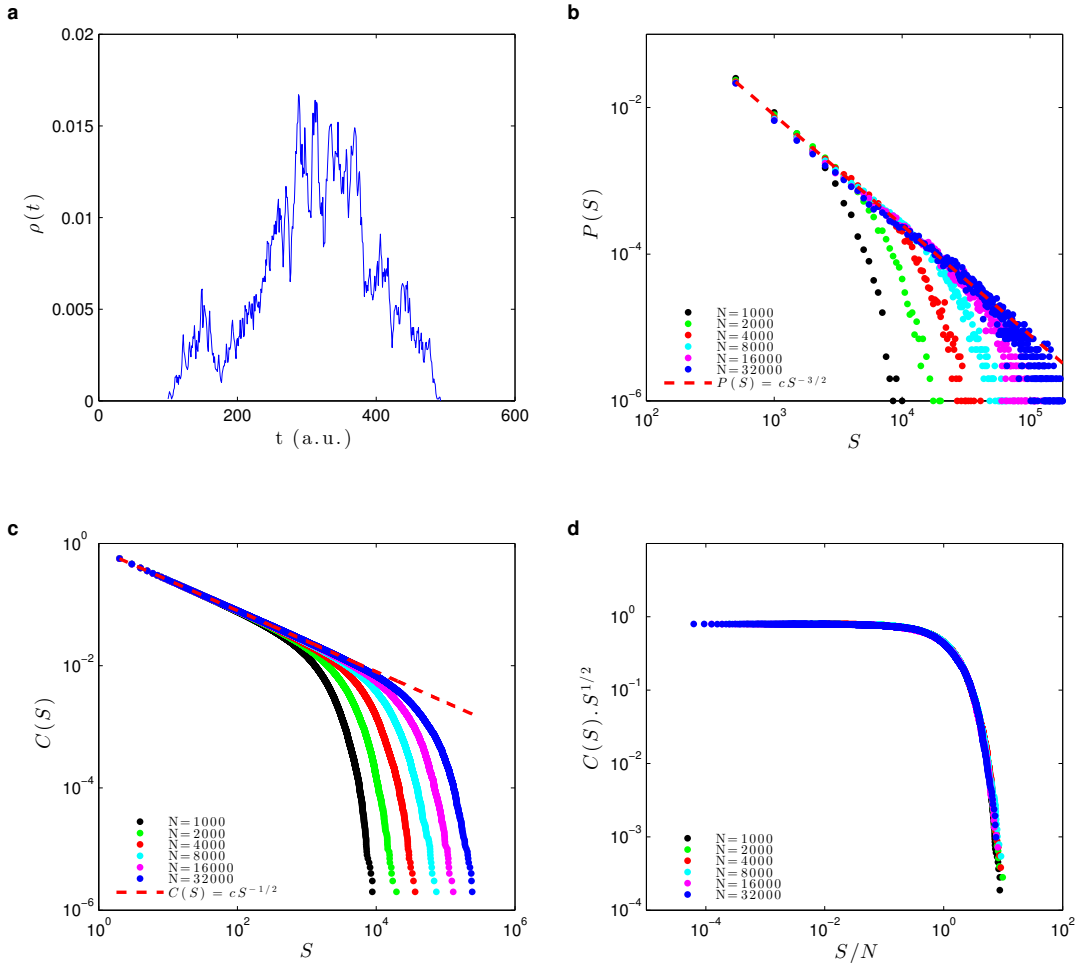

FIG. 5: a) Example of avalanche profile $\rho[t]$ at the critical point $W_c = 1, \gamma = 1$ with $\mu = 1/2$. The size of an avalanche is $S = N\sum_{t=a}^{b}\rho[t]$ where $t_i = a$ and $t_f = b$ are the initial and final times of the avalanche, respectively. The duration of the avalanche is $D = b - a$. b) Histogram of the probability $P(S)$ for an avalanche of size S, for network sizes $N = 1000, 2000, 4000, 8000$ and 16000. The line proportional to $S^{-\beta}$, with $\beta = 3/2$ is a guide to the eye. c) Complementary cumulative function $C(S) = \sum_{S}^{\infty} P(S)dS$ with the previous network sizes. This function gives the probability of occurring an avalanche greater than S. Being an integral of $P(S)$, its power law exponent is $-\beta + 1 = -1/2$. d) Finite size scaling (data collapse for different N) for $C(S, N)$, giving the N independent curve $g = S^{1/2}C(S/N_S^c)$. The cutoff exponent is $c_S = 1$.

We also studied the distribution of avalanche duration $P(D)$, as a function of N (Fig. 6). We obtained $P(D) \propto D^{-\delta}$ with $\delta = 2$ and a cutoff exponent $c_D = 1/2$, in accord with the literature [10].

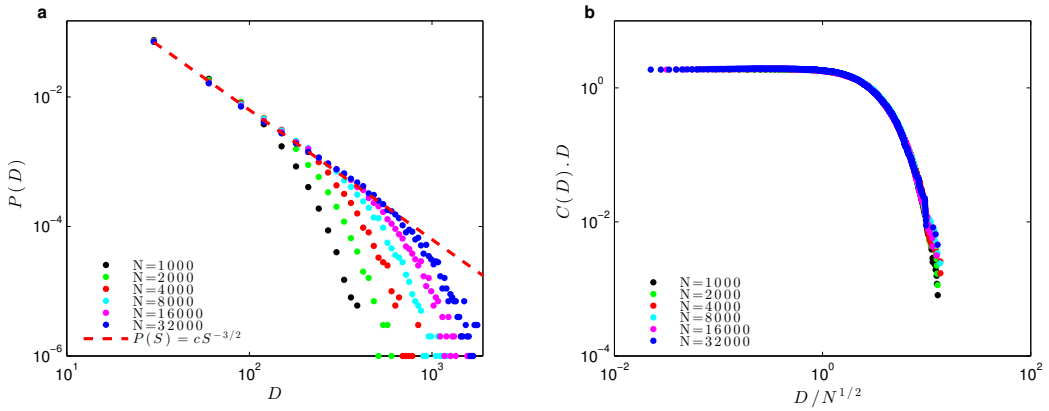

FIG. 6: a) Mean duration $< D >$ of avalanches at the critical point $W_C = 1, \mu = 1/2$ for network sizes $N = 1000, 2000, 4000, 8000$ and 16000. b) Histogram of the probability $P(D)$ for an avalanche of duration D, for different network sizes. The line proportional to $D^{-\delta}$, with $\delta = 2$ is a guide to the eye. c) Complementary cumulative function $C(D) = \sum_D^\infty P(D)dD$ with the previous network sizes. This function gives the probability of occurring an avalanche greater than D. Being an integral of $P(D)$, its power law exponent is $-\delta + 1 = -1$. d) Finite size scaling (data collapse for different N) for $C(D, N)$, giving the N independent curve $g_D = C(D/N_D^c)$. The cutoff exponent is also $c_D = 1/2$.

E. The model with dynamic parameters

The results of Section III D were obtained by fine-tuning the network at the critical line $\gamma W = \gamma_C W_C = 1$. If the critical region has some advantage, then we must present a homeostatic mechanism that could tune such biological networks to the criticality.

One way to implement this idea is to let the weights W_{ij} evolve with time, in a way that mimics the observed loss of strength after a synaptic discharge (presumably due neurotransmitter vesicles depletion), and the subsequent slow recovery [9, 10, 30, 31]. However, since the relevant parameter for criticality in the GL model is γW, we propose instead to work with dynamic gains $\gamma_i[t]$ while keeping the W_{ij} fixed. The idea is to reduce the gain $\gamma_i[t]$

when the activity is too large, and let it recover towards a higher resting value when it is too low:

$$\gamma_i[t+1] = (1 - \epsilon - \nu X_i[t])\gamma_i[t] + \epsilon\Gamma \; . \tag{14}$$

Here the factor $\epsilon = e^{-\theta\Delta}$ is related to the characteristic recovery time θ for the gain, Γ is the resting (maximum) gain, and $\nu \in [0, 1]$ is the fraction of gain lost due the discharge. This model is plausible biologically, since it mimics the well known phenomenon of *spike adaptation* [34, 35].

This approach seems sufficient to achieve self-organized criticality. Fig. 7a shows a simulation where the average gain $\gamma[t] = (\sum_{i=1}^{N} \gamma_i[t])/N$ tends towards the critical value $\gamma_{\mathsf{C}}(W) = 1/W$, starting from $\gamma[0] \neq 1$. The avalanche size distributions (Fig. refSOCb) and the finite-size scaling (Fig. 7c) are well behaved. A curious result is that the cutoff exponent is now $c_S = 2/3$ which differs from the static case ($c_S = 1$).

FIG. 7: (a) Self-organization to criticality of the average gain $\gamma[t]$ by using dynamical neuronal gains $\gamma_i[t]$ starting from different initial conditions, with $\gamma_i[0] \in [0, \gamma_{max}]$ so that the average gain is $\gamma[0] = \gamma_{\max}/2$. The horizontal dashed line is the value $\gamma_{\mathsf{C}} = 1$. (b) Avalanche size distribution $P(S)$ for several N. The solid line $S^{3/2}$ is a guide to the eyes. (c) Data collapse of the complementary accumulated function $g = S^{1/2}C(S/N_S^c)$. The cutoff exponent is $c_S = 2/3$.

IV. CONCLUSIONS AND PERSPECTIVES

a. Stochasticity in the model: According to our analysis and simulations, the GL stochastic neuron model introduced by Galves and Löcherbach [20, 21] seems to be adequate for neuronal network studies. The LSIF models of Soula *et al.* [16] and Cessac [17–19] introduce stochasticity in the neuron's behavior by adding noise terms to its potential, whereas the GL model makes the firing a stochastic phenomenon with potential-dependent probability $\Phi(V)$.

The two models yield similar neuron and network behavior, but are not entirely equivalent, because the integration of the noise terms makes the Soula and Cessac neurons less deterministic with time. However, this difference is very subtle. With an appropriate choice of parameters, the GL model should mimic the network behavior as the noisy input ones, and vice-versa.

b. Phase transitions: In particular, networks of GL neurons display a variety of dynamical states with interesting phase transitions. We looked for stationary regimes in such networks, for some specific firing functions Φ with no spontaneous activity at the baseline potential (that is, with $\Phi(0) = 0$). We studied the changes in those regimes as a function of the mean synaptic gain W. We found basically tree kinds of phase transitions [26–28]: first order (discontinuous) absorbing transitions when $\Phi'(0) = 0$, a ceaseless dynamic regime with no phase transitions when $\Phi'(0) = +\infty$, and second order (continuous) absorbing phase transitions when $0 < \Phi'(0) < +\infty$.

The model studied by Larremore *et al.* [23] is equivalent to the GL model with monomial firing function and $r = 1$. They did not report any phase transition (perhaps because of the the inhibitory neurons in their network), but found a ceaseless activity very similar to what we observed in monomial GL model with $r < 1$.

The deterministic IF neuron models do not seem allow these kinds of transitions are not possible with deterministic IF neurons [5, 13, 14]. Perhaps, a stochastic firing function $Phi(V)$ is a necessary ingredient to this kind of transitions.

c. Avalanches: In the case of second-order phase transitions (such as with monomial Φ and $r = 1$), we detected firing avalanches at the critical parameter settings, whose size distribution follows the expected power law.

d. Self-organized criticality: Inspired by the analysis of phase transitions, we proposed a new mechanism for short-scale neuronal network plasticity, based on dynamically varying neuron gains $\gamma_i[t]$ instead of dynamic synaptic weights as proposed by other authors [9, 10, 30, 31]. This new mechanism is biologically plausible and was found to be sufficient to obtain self-organized criticality. Its great advantage is computational efficiency: when simulating N neurons with K synapses each, there are only N dynamic equations for the gains $\gamma_i[t]$, instead of NK equations for the synaptic weights $W_{ij}[t]$.

e. Directions for future research: Future research could investigate other network topologies and firing functions, heterogeneous networks, the effect of inhibitory neurons [13, 23], and network learning. The study of the self-organized criticality with GL neurons and dynamic neuron gains is particularly promising.

V. ACKNOWLEDGMENTS

This was an activity of the the FAPESP Center for Neuromathematics (FAPESP grant 2013/07699-0). OK and AAC also received support from CNAIPS-USP and FAPESP. LB and JS also received CNPq support (grants 165828/2015-3 and 310706/2015-7).

---

[1] Lapicque, L. Recherches quantitatives sur l'excitation électrique des nerfs traitée comme une polarisation. J. Physiol. Pathol. Générale **9**, 620–635 (1907). Translation: Brunel, N. & van Rossum, M.C. Quantitative investigations of electrical nerve excitation treated as polarization. Biol. Cybernetics **97**, 341–349 (2007).

[2] Burkitt, A.N. A Review of the Integrate-and-fire Neuron Model: I. Homogeneous Synaptic Input. Biol. Cybernetics **95**, 1–19 (2006).

[3] Burkitt, A. N. A review of the integrate-and-fire neuron model: II. In-homogeneous synaptic input and network properties. Biol. Cybernetics **95**, 97–112 (2006).

[4] Naud, R. & Gerstner, W. The performance (and limits) of simple neuron models: generalizations of the leaky integrate-and-fire model. *Computational Systems Neurobiology* 163–192 (Springer, New York, 2012).

[5] Brette, R., Rudolph, M., Carnevale, T., Hines, M., Beeman, D., Bower, J. M., ... & Destexhe, A. Simulation of networks of spiking neurons: a review of tools and strategies. J. Comput. Neurosci. **23**, 349–398 (2007).

[6] Brette, R. What is the most realistic single-compartment model of spike initiation?. PLoS Comput. Biol. **11**, e1004114 (2015).

[7] Buonocore, A., Caputo, L., Pirozzi, E. & Carfora, M.F. A leaky integrate-and-fire model with adaptation for the generation of a spike train. Math. Biosci. Engineer. **13**, 483–493 (2016).

[8] Beggs, J.M. & Plenz, D. Neuronal avalanches in neocortical circuits. J. Neurosci. **23**, 11167–11177 (2003).

[9] Levina, A., Herrmann, J. M. & Geisel, T. Dynamical synapses causing self-organized criticality in neural networks. Nat. Phys. **3**, 857–860 (2007).

[10] Bonachela, J.A., De Franciscis, S., Torres, J.J. & Muñoz, M.A. Self-organization without conservation: are neuronal avalanches generically critical?. J. Stat. Mech. **2010**, P02015 (2010).

[11] Benayoun, M., Cowan, J.D., van Drongelen, W. & Wallace, E. Avalanches in a stochastic model of spiking neurons. PLoS Comput. Bio. **6**, e1000846 (2010).

[12] Izhikevich, E. M. Simple Model of Spiking Neurons. IEEE Trans. on Neural Networks **14**(6), 1569–1572.

[13] Ostojic, S. Two types of asynchronous activity in networks of excitatory and inhibitory spiking neurons. Nat. Neurosci. **17**, 594–600 (2014).

[14] Torres, J.J. & Marro, J. Brain Performance versus Phase Transitions. Sci. Reports **5**, 12216 (2015).

[15] Mcdonnell, M.D., Goldwyn, J.H. & Lindner, B. Neuronal stochastic variability: influences on spiking dynamics and network activity. Front. Comput. Neurosci. **10**, 38 (2016).

[16] Soula, H., Beslon, G. & Mazet, O. Spontaneous dynamics of asymmetric random recurrent spiking neural networks. Neural Comput. **18**, 60–79 (2006).

[17] Cessac, B. A discrete time neural network model with spiking neurons. J. Math. Biol. **56**, 311–345 (2008).

[18] Cessac, B. A view of neural networks as dynamical systems. Int. J. Bifurcation and Chaos **20**, 1585–1629 (2010).

[19] Cessac, B. A discrete time neural network model with spiking neurons II: Dynamics with noise. J. Math. Biol. **62**, 863–900 (2011).

[20] Galves, A. & Löcherbach, E. Infinite systems of interacting chains with memory of variable length — a stochastic model for biological neural nets. J. Stat. Phys. **151**, 896–921 (2013).

[21] Galves, A. & Löcherbach, E. Modeling networks of spiking neurons as interacting processes with memory of variable length. arXiv preprint: 1502.06446 (2015).

[22] De Masi, A., Galves, A., Löcherbach, E. & Presutti E. Hydrodynamic limit for interacting neurons. J. Stat. Phys. **158**, 866–902 (2015).

[23] Larremore, D.B., Shew, W.L., Ott, E., Sorrentino, F. & Restrepo, J.G. Inhibition causes ceaseless dynamics in networks of excitable nodes. Phys. Rev. Lett. **112**, 138103 (2014).

[24] Cooper, S. J. Donald O. Hebb's synapse and learning rule: a history and commentary, Neurosci. & Biobehav. Rev. **28**, 851–874 (2005).

[25] Tsodyks, M., Pawelzik, K. & Markram, H. Neural networks with dynamic synapses. Neural Comput. **10**, 821-835 (1998).

[26] Kinouchi, O. & Copelli, M. Optimal dynamical range of excitable networks at criticality. Nat.

Phys. **2**, 348–351 (2006).

[27] Larremore, D.B., Shew, W.L. & Restrepo, J.G. Predicting criticality and dynamic range in complex networks: effects of topology. Phys. Rev. Lett. **106**, 058101 (2011).

[28] Hesse, J. & Gross, T. Self-organized criticality as a fundamental property of neural systems. Front. Systems Neurosci. **8**, 166 (2014).

[29] Massobrio, P., de Arcangelis, L., Pasquale, V., Jensen, H.J., & Plenz, D. Criticality as a signature of healthy neural systems. Frontiers Syst. Neurosci. **9**, 22 (2015).

[30] Costa, A.A., Copelli, M., and Kinouchi, O. Can dynamical synapses produce true self-organized criticality?. J. Stat. Mech. **2015**, P06004 (2015).

[31] Campos, J.G.F., Costa, A.A., Copelli, M. & Kinouchi, O. Differences between quenched and annealed networks with dynamical links. in preparation (2016).

[32] Girardi-Schappo, M., Tragtenberg, M.H.R. & Kinouchi, O. A brief history of excitable map-based neurons and neural networks. J. Neurosci. Meth. **220**, 116–130 (2013).

[33] Ibarz, B., Casado, J.M. & Sanjuán, M.A.F. Map-based models in neuronal dynamics. Phys. Reports **501**, 1–74 (2011).

[34] Ermentrout, B., Matthew, P. & Boris, G. The effects of spike frequency adaptation and negative feedback on the synchronization of neural oscillators. Neural Comput. **13**, 1285–1310 (2001).

[35] Benda, J. & Herz, A.V.M. A universal model for spike-frequency adaptation. Neural Comput. **15**, 2523–2564 (2003).

[36] Lipetz, L.E. The relation of physiological and psychological aspects of sensory intensity. W. R. Lowenstein (Ed.), *Handbook of sensory physiology* Vol. 1, 191–225 (Springer-Verlag, New York, 1971).

[37] Naka, K.I., & Rushton, W.A.H. (1966). S-potentials from luminosity units in the retina of fish (cyprinidae). J. Physiol. **18**, 587–599 (1966).

VI. METHODS

The avalanche statistics were obtained by simulating the evolution of a finite network of N neurons, with uniform synaptic strengths $W_{ij} = W$ (except $W_{ii} = 0$) and critical parameter values. Each avalanche was started with all neuron potentials $V_i[0] = V_{\mathsf{R}} = 0$ and

forcing the firing of a single neuron by setting $X_i[0] = 1$. The network was then simulated according to Eq. (1) until all activity ceased and all potentials had decayed to such low values that further firings would not be expected for thousands of steps.

VII. SUPPLEMENTARY INFORMATION

A. Details of the mean-Field analysis

In the mean-field analyses reported in this article, we assume that the synaptic weights follow a distribution with average W and finite variance, and that the output axon of each neuron makes synapses with all other neurons. The mean-field approximation disregards correlations, so the final term of Eq. (1) becomes:

$$\frac{1}{N}\sum_{j=1}^{N} W_{ij} X_j[t] = W\rho[t]\,. \tag{15}$$

Notice that the variance of the weights W_{ij} becomes immaterial when N tends to infinity.

In this analysis we also assume that the external inputs $I_i[t]$ are zero for all neurons and all times. Therefore, every neuron i that does not fire between t and $t+1$ (that is, with $X_i[t] = 0$) has its potential changed in the same way:

$$V_i[t+1] = \mu V_i[t] + W\rho[t]\,, \tag{16}$$

Recall that the distribution $P[V,t]$ had a Dirac impulse at potential $U_0 = V_\mathsf{R}$, representing all neurons that fired in the previous interval. This Dirac impulse is modified in later steps by Eq. (16). It follows that, once all neurons have fired at least once, the distribution $P[V,t]$ will be a combination of discrete impulses with amplitudes $\eta_0[t], \eta_1[t], \eta_2[t], \ldots$, at potentials $U_0[t], U_1[t], U_2[t], \ldots$, such that $\sum_{k=0}^{\infty} \eta_k = 1$ See Fig. 12.

The amplitude $\eta_k[t]$ is the fraction of neurons with *firing age* k at discrete time t; that is, neurons that fired between times $t-k-1$ and $t-k$, and did not fire between $t-k$ and t. The common potential of those neurons, at time t, is $U_k[t]$. In particular, $\eta_0[t]$ is the fraction $\rho[t-1]$ of neurons that fired in the previous time step, between discrete times $t-1$ and t; and $U_0[t]$ is always V_R. For this type of distribution, the integral of Eq. (3) becomes a discrete sum:

$$\rho[t] = \sum_{k=0}^{\infty} \Phi(U_k[t])\eta_k[t]\,. \tag{17}$$

According to Eq. (16), the values $\eta_k[t]$ and $U_k[t]$ evolve by the equations

$$\eta_0[t+1] \;=\; \rho[t] \tag{18}$$

$$U_0[t+1] \;=\; V_{\mathsf{R}}\,, \tag{19}$$

$$\eta_k[t+1] \;=\; (1 - \Phi(U_{k-1}[t]))\,\eta_{k-1}[t]\,, \tag{20}$$

$$U_k[t+1] \;=\; \mu U_{k-1}[t] + W\rho[t]\,, \tag{21}$$

for all $k \geq 1$.

B. Stationary phases for general Φ and μ

In the context of mean-field analysis, a *stationary phase* is a potential distribution $P(V)$ of membrane potentials that does not change with time. In such a regime, quantities U_k and η_k do not depend on the time t. Therefore, the evolution equations (18–21) become a pair of recurrence equations:

$$\eta_0 \;=\; \rho = \sum_{k=0}^{\infty} \Phi(U_k)\eta_k\,, \tag{22}$$

$$U_0 \;=\; 0\,, \tag{23}$$

$$\eta_k \;=\; (1 - \Phi(U_{k-1}))\,\eta_{k-1}\,, \tag{24}$$

$$U_k \;=\; \mu U_{k-1} + W\rho\,, \tag{25}$$

for all $k \geq 1$. Since equations 22) and (24) are homogeneous on the η_k, the normalization condition $\sum_{k=0}^{\infty} \eta_k \;=\; 1$ must be included explicitly.

In some special cases, the solution has a closed analytic formula. For example, when $\mu = 0$, Equations 25 reduce to Eq.(6). Otherwose, Eqs. (22–25) can be solved numerically, e. g. by simulating the evolution of the potential distribution $P[V,t]$ according to Equation. (18–21), starting from an arbitrary initial distribution, until reaching a stable distribution. (The probabilities η_k should be renormalized for unit sum after each time step, to compensate for rouding errors.)

We used this method to explore numerically the (W,ρ) and (W,γ) phase diagrams for various values of $\mu > 0$, for the monomial firing function with $V_{\mathsf{T}} = 0$ and $r = 1$ and γ. See Fig. 8. Only the first 100 peaks (U_k, η_k) were considered, since, for the given μ and Φ, there was no significant probability beyond that point.

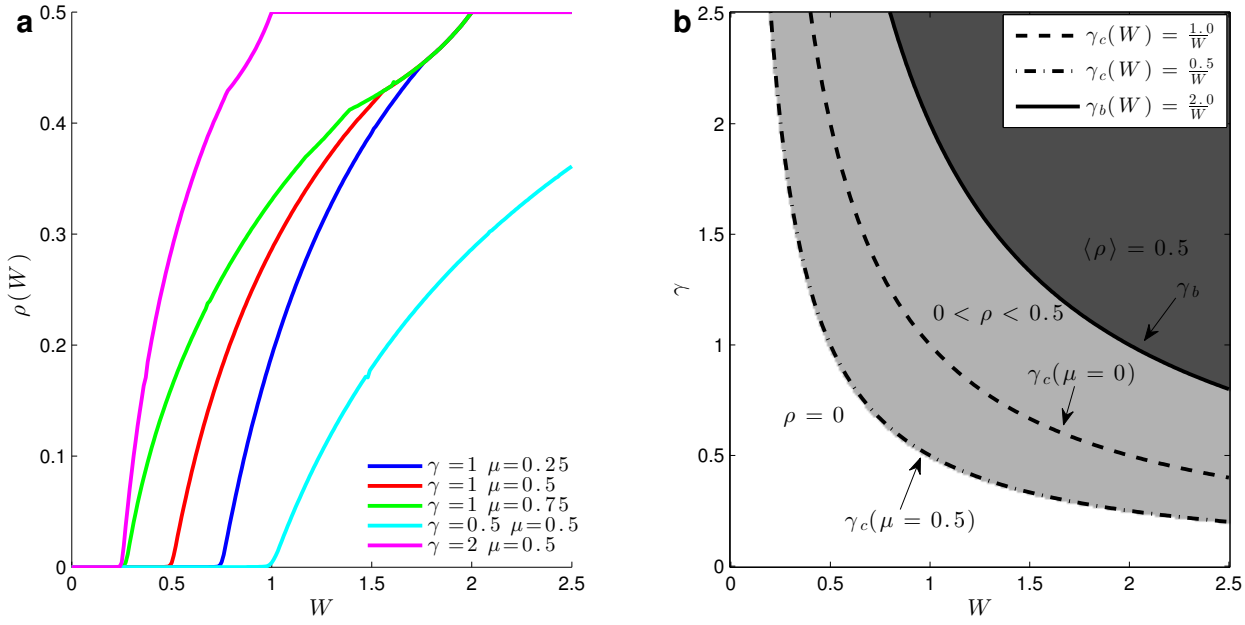

FIG. 8: a) Numerically computed (W, ρ) diagrams for the monomial firing function with $r = 1$ and $(\gamma, \mu) = (1, 1/4), (1, 1/2), (1, 3/4), (1/2, 1/2), (2, 1/2)$. b) Numerically computed (W, γ) diagram for showing some critical lines $\gamma_{\mathsf{C}}(W) = (1-\mu)/W$ and the bifurcation line $\gamma_{\mathsf{B}}(W) = 2/W$ to 2-cycles.

When $\mu > 0$, the critical line in the (W, γ) diagram becomes $\gamma_{\mathsf{C}}(W) = (1-\mu)/W$, or $W_{\mathsf{C}}(\gamma) = (1-\mu)/\gamma$. See Fig. 8b. For W just above W_{C}, we have $\rho(W) \approx C(W - W_{\mathsf{C}})/W$ for some constant $C > 0$. The mean-field critical exponent is therefore $\alpha = 1$, characteristic of the directed percolation (DP) universality class [26, 28] – as in the case $\mu = 0$.

C. Mean-field analysis with rational Φ and $\mu = 0$

In this section we provide additional details of the mean-field analysis with rational firing functions, Eq (12), with $\mu = 0$ and $V_{\mathsf{T}} = V_{\mathsf{R}} = 0$. Recall that there are no degenerate stationary regimes or 2-cycles, since these functions never saturate ($W_{\mathsf{B}} = 2V_{\mathsf{S}} = +\infty$).

a. The case $r = 1$: With $V_{\mathsf{T}} = 0$ and $r = 1$, the rational firing function is

$$\Phi(V) = \frac{\gamma V}{1 + \gamma V}\,. \tag{26}$$

In this case, Eq. (5) becomes:

$$2\gamma W\rho^2 + (1 - \gamma W)\rho = 0\,. \tag{27}$$

We then have a phase transition given by:

$$\rho = \frac{W - W_{\mathsf{C}}}{2W} = \frac{\gamma - \gamma_{\mathsf{C}}}{2\gamma} \tag{28}$$

with $W_{\mathsf{C}}(\gamma) = 1/\gamma$ or $\gamma_{\mathsf{C}}(W) = 1/W$. See Fig. RhoxWratb. So, the critical line is the same of the monomial model (Fig. 1c).

b. The case $r > 1$: The density of firing neurons is given by:

$$2(\gamma W)^r \rho^r - (\gamma W)^r \rho^{r-1} + 1 = 0\,. \tag{29}$$

The discontinuous phase transitions occur when W_{C} does not admit a value $\rho > 0$. For example, with $r = 2$ we have:

$$\rho = \frac{\gamma W + \sqrt{(\gamma W)^2 - 8}}{4\gamma W}\,, \tag{30}$$

which is well behaved and tends to $\rho \to 1/2$ when $W \to \infty$. However there is no solution for $W < W_{\mathsf{C}} = \frac{\sqrt{8}}{\gamma}$ and at this point there is a discontinuous transition, with a step $\rho_{\mathsf{C}} = 1/4$. In general the step $\rho_{\mathsf{C}}(r)$ diminishes with r and we recover $\rho_{\mathsf{C}} = 0$ for $r = 1$ (Fig. 2b).

D. Isolated neurons

In this section we analyze the behavior of the GL neuron model under the standard experiment where an isolated neuron in vitro is artificially injected with a current of constant intensity J. That corresponds to setting the external input signal $I_1[t]$ of that neuron to a constant value $I = J\Delta/C$ where C is the effective capacitance of the neuron.

⋆Ainda acho que não precisa dessa $F(I)$***. Estamos analisando o comportamento do modelo; não tem que ajustar nada com experimentos. A firing rate do modelo é a própria*** ρ ***do campo médio, sem nenhum fator multiplicador, por este argumento:*** An isolated neuron will fire at a stable firing rate (average number of firings per sampling step) ρ if and only if ρ is the mean-field firing ratio of an infinite network of neurons, all with constant external input term I but no synaptic inputs. ***⋆Então, wue tal isto:***

The time-averaged firing rate (average number of firings per sampling step) of the isolated neuron can be derived in the same way as the firing ratio ρ of mean-field analysis. Namely:

$$\rho = \Phi(I)(1 - \rho)\,, \tag{31}$$

For the monomial firing function, while $I < V_{\mathsf{S}} = 1/\gamma$, we have:

$$\rho = \frac{(\gamma I)^r}{1 + (\gamma I)^r} \,, \tag{32}$$

which is less than 1/2. For any $I \geq 1/\gamma$ the firing rate saturates at $\rho = 1/2$ (the neuron fires at every other step, alternating between potentials $U_0 - V_{\mathsf{R}} = 0$ and $U_1 = I$.

For the rational function we have:

$$\rho = \frac{(\gamma I)^r}{1 + 2(\gamma I)^r} \,, \tag{33}$$

which goes to $\rho \to 1/2$ only for $I \to \infty$ (Fig. 9).

In either case there are no phase transitions. Interestingly, Eqs. (e.rho.isolin) and (e.rho.isorat), know as Michaelis-Menten functions, are frequently used to fit the (normalized) firing response of biological neurons to constant input currents [36, 37].

⋆[stolfi:] Não tem phase transitions porque $\mu = 0$ ***e*** $V_{\mathsf{T}} = 0$***. Nesse caso o experimento de injeção de corrente fica muito bobo: o efeito do*** I ***equivale a deslocar o gráfico da*** Φ ***para a esquerda, causando*** $\Phi(0) > 0$***. Nos slides da minha palestra tem o caso*** $\mu > 0$***,*** $V_{\mathsf{T}} > 0$***, e lá aparecem regimes diferentes – mas com transição bem gradual.***

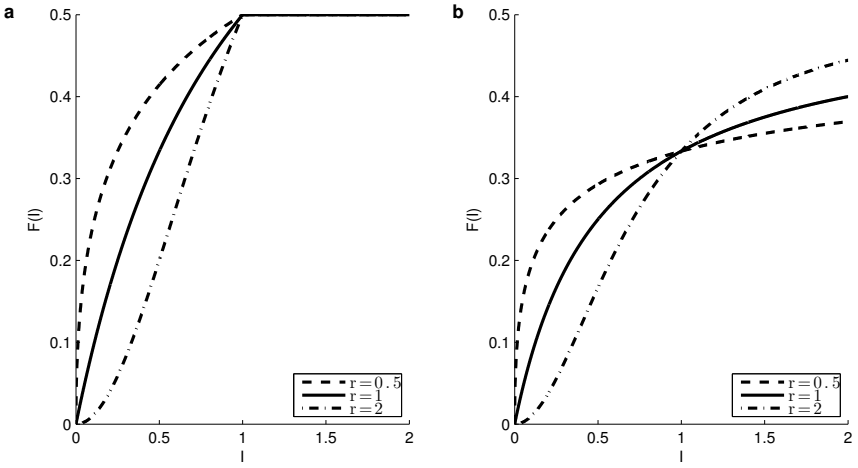

FIG. 9: Firing rate of an isolated neuron with (a) monomial firing function and (b) rational firing function, as a function of external input I, for exponents $r = 0.5, 1$.

E. The case with threshold $V_\mathsf{T} > 0$

The standard IF model has $V_\mathsf{T} > 0$. If we allow this feature in our models we find a new ingredient that produces first order phase transitions. Indeed, in this case, if $U_1 = W\rho + I < V_\mathsf{T}$ then we have a single peak at $U_0 = 0$ with $\eta_0 = 1$, which means we have a silent state. When $U_1 = W\rho + I > V_\mathsf{T}$, we have a peak with height $\eta_1 = 1 - \rho$ and $\rho = \eta_0 = \Phi(U_1)\eta_1$. For the linear monomial model this leads to the equations:

$$\rho = \gamma(U_1 - V_\mathsf{T})(1 - \rho)\,, \tag{34}$$

$$\gamma W\rho^2 + (1 - \gamma W - \gamma V_\mathsf{T} + \gamma I)\rho + \gamma V_\mathsf{T} - \gamma I = 0\,, \tag{35}$$

$$\rho = \frac{(\gamma W + \gamma V_\mathsf{T} - \gamma I - 1) + \sqrt{(\gamma W + \gamma V_\mathsf{T} - \gamma I - 1)^2 - 4\gamma^2 W V_\mathsf{T} + 4\gamma^2 W I}}{2\gamma W}\,. \tag{36}$$

This solution exists only for γW values such that:

$$\gamma(W + V_\mathsf{T} - I) - 1 > 2\gamma\sqrt{W(V_\mathsf{T} - I)}. \tag{37}$$

This produces the condition:

$$\gamma W > \gamma W_\mathsf{C} = \left(1 + \sqrt{\gamma(V_\mathsf{T} - I)}\right)^2\,, \tag{38}$$

which defines a first order critical line. At the critical line the density of firing neurons is:

$$\rho_\mathsf{C} = \frac{\sqrt{\gamma(V_\mathsf{T} - I)}}{1 + \sqrt{\gamma(V_\mathsf{T} - I)}}\,, \tag{39}$$

which is nonzero (discontinuous) for any $V_\mathsf{T} > I$. These transitions can be seen in (Fig. 10). The solutions for Eqs. (36) and (39) is also valid only for $\rho_\mathsf{C} < 1/2$ (2-cycle bifurcation). This imply the maximal value $V_\mathsf{T} = 1/\gamma - I$.

The rational model also enables analytic solution. By following the same method we obtain:

$$\rho = \frac{2\gamma(V_\mathsf{T} - I) + \gamma W - 1 + \sqrt{(2\gamma(V_\mathsf{T} - I) + \gamma W - 1)^2 - 8\gamma^2 W(V_\mathsf{T} - I)}}{4\gamma W}\,, \tag{40}$$

$$\gamma W_\mathsf{C} = \left(1 + \sqrt{2\gamma(V_\mathsf{T} - I)}\right)^2\,, \tag{41}$$

$$\rho_\mathsf{C} = \frac{1}{2}\,\frac{\sqrt{2\gamma(V_\mathsf{T} - I)}}{1 + \sqrt{2\gamma(V_\mathsf{T} - I)}}\,. \tag{42}$$

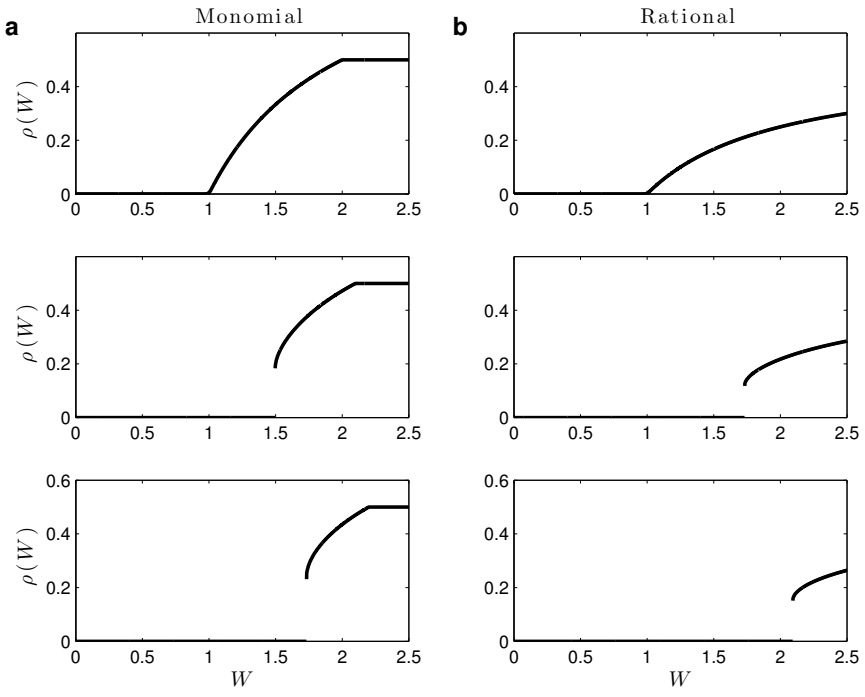

FIG. 10: Phase transitions for the $r = 1$ a) monomial model and b) rational model, with $\gamma = 1$ and thresholds $V_\mathsf{T} = 0, 0.1, 0.5$ and 0.9. The discontinuity ρ_C goes to zero for $V_\mathsf{T} \to 0$.

Since $\rho_\mathsf{C} \to 1/2$ only for $V_\mathsf{T} \to \infty$, we have no bifurcation to 2-cycles in the rational model. Also notice that the solution is valid only for $V_\mathsf{T} > I$, with a discontinuous phase transition with $\rho_\mathsf{C} > 0$.

Similar results (discontinuous phase transitions with $V_\mathsf{T} > 0$) can be numerically obtained for the $r \neq 1$ cases, both for the monomial and rational models.

VIII. JUNK

A. Cycles of period 2

⋆Esta seção estava dentro da seção "isolated neuron". Parece supérflua, já que estes ciclos (e seu diagrama de fase) são exatamente os mesmos do LIF determinístco, ou qualquer Φ ***que satura. O texto principal já diz tudo o que há para dizer. Além disso, com*** $\mu > 0$ ***e*** V_T ***suficientemente grande (situação realista?) aparecem*** p***-ciclos para*** $p > 2$***. Proponho tirar esta seção***

Cycles of period 2 appear for $\Phi(V)$ functions that have a plateau $\Phi(V) = 1$ above some V_{S}. For example, the monomial function (for any r) has a plateau for $V > V_{\mathsf{T}} + 1/gamma$.

In the case $r = 1, \mu = 0, V_{\mathsf{T}} = 0$, $V = W\rho$ and the 2-cycles bifurcation occur at $\rho = 1/2$ so that When $W > W_{\mathsf{B}} = 2/\gamma$, we have $\Phi(V) = 1$. From this point all the neurons of the peak $U_1[t] = W\rho[t] > 1/\gamma$ (with density $\eta_1[t]$) fire together creating in the next step the peak $\eta_0[t+1] = \eta_1[t]$, and the previous peak $\eta_0[t]$ goes to the position $U_1[t+1]$ creating $\eta[t+1] = \eta[t]$. Since $\rho[t] = \eta_0[t]$, we have a 2-cycle $\rho[t+1] = 1 - \rho[t]$ where the amplitudes differ (they are equal, $\rho[t+1] = \rho[t] = 1/2$ only at the bifurcation point.

These 2-cycles are somewhat anomalous regimes: they have marginal stability and have no attraction basin. That is, if the initial condition is put as $\rho[t=0] = \eta_a > 1/2$, then in the next step we have $\rho[t=1] = \eta_b = 1 - \eta_a < 1/2$ and the network goes back to the initial state.

The values for η_a, η_b are not unique for a given W (as would be the case of a 2-cycle with an attractor basin), but can assume any value inside an interval $[\eta_{max}(W), \eta_{min}(W)]$ where $\eta_{min} = 1 - \eta_{max}(W)$. We can determine these values from the condition $U_1 = W\eta_{min}$ is situated at the beginning of the plateau at $V = 1/\gamma$, that is, $\eta_{min} = 1/(\gamma W)$ and $\eta_{max} = (\gamma W - 1)/(\gamma W)$ (Fig. 11).

For functions $\Phi(V)$ that do not have plateaus, like the rational model, such 2-cycles are not stationary phases. However, for large W such that $\Phi(V) \approx 1$, transient 2-cycles appear. Since transient synchronized oscillations have been observed in some biological networks, it could be that these 2-cycles of our models have some biological meaning. Their frequency is given by $f = 2/\delta t$, where Δt is the inverse of our discrete time step, a free parameter that could be adjusted to the experimental data.

B. The case $\mu > 0$

Models with any function $\Phi(V)$ can be solved numerically from the general schema given by Eqs. (**??**). Similarly to the case $\mu = 0$, what determines the nature (or absence) of a phase transition is the exponent r that dominates the low V behavior of $\Phi(V)$. As before, if $r < 1$, we have $W_{\mathsf{C}} = 0$ and if $r > 0$ (or $V_{\mathsf{T}} > 0$) we have a discontinuous phase transitions. In the $r = 1$ case, we have a continuous phase transition. This will be fully explored in another paper. Here we only report the monomial case with $r = 1$ and general μ because it

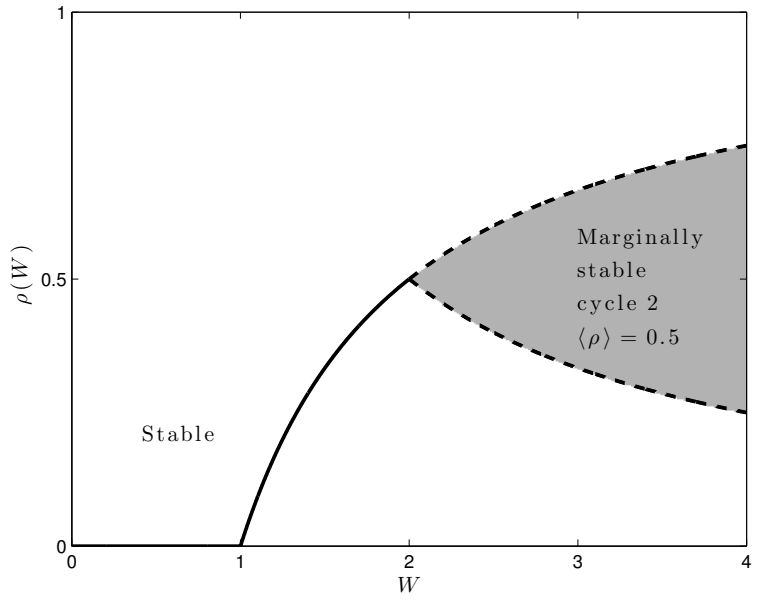

FIG. 11: Marginally stable 2-cycles appear at $W_{\mathsf{B}} = 2/\gamma$ (here $\gamma = 1$). They can have any value satisfying $\rho[t+1] = 1-\rho[t]$ between the extreme values $\eta_{max} = (\gamma W-1)/(\gamma W)$ and $\eta_{min} = 1/(\gamma W)$ (dashed lines).

allows some analytic results.

We consider the firing function $\phi(V) = \gamma V$ for $0 < V < 1/\gamma$ and $\phi(V) = 1$ for $V > 1/\gamma$. With this $\Phi(V)$, Eqs. (3) simplify to two cases. If there is a peak n at $U_n > 1/\gamma$ we get:

$$\rho = \gamma \sum_{k=1}^{n-1} U_k \eta_k + \eta_n \,, \tag{43}$$

but if all peaks are below $V = 1/\gamma$ we write:

$$\rho = \gamma \sum_{k=1}^{\infty} U_k \eta_k \,. \tag{44}$$

We also have:

$$\eta_k \;=\; (1 - \gamma U_{k-1})\, \eta_{k-1} \,, \tag{45}$$

$$U_k \;=\; \mu U_{k-1} + W\rho \,, \tag{46}$$

So, the solution of Eq. (43) depends on the number of peaks below $U = 1/\gamma$ and the single peak with $U_n > 1/\gamma$ (with this $\Phi(U)$, the $(1 - \Phi(U_n) = 0$ term kills all superior peaks with $k > n$) (Fig. 12).

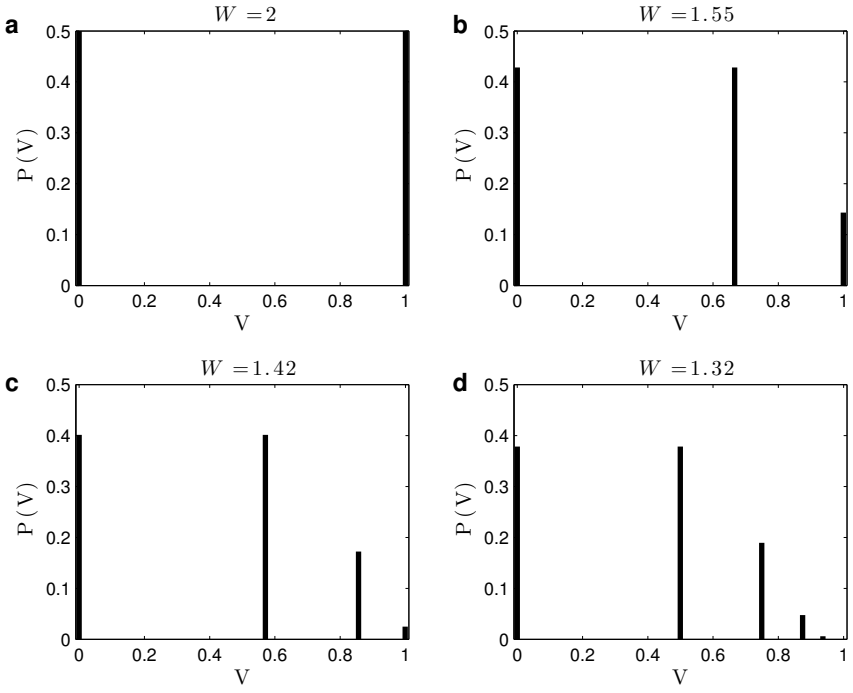

FIG. 12: Examples of stationary potential distributions $P(V)$ for the monomial $r = 1$ case with different values of W and $\mu = 1/2, \gamma = 1$. a) $W_2 = W_{\mathsf{B}} = 2$, two peaks; b) $W_3 = \frac{14}{9}$, three peaks; c) $W_4 = \frac{488}{343}$, four peaks, d) $W_\infty \approx 1.32$, infinite number of peaks with $U_\infty = 1$. Notice that for $W < W_\infty$ all the peaks in the distribution $P(V)$ lie at potentials $U_k < 1/\gamma$. For $W_{\mathsf{B}} = 2$ we have $\eta_0 = \eta_1 = 1/2$, producing a bifurcation to a 2-cycle.

Lets start with the simple case where there are only two peaks, one at $U_0 = 0$ with density η_0 and the other ($n = 1$) peak exactly at $U_1 = 1/\gamma$ with density η_1. In this case, Eq. (**??**) tell us that $\rho = \eta_1$, that is, $\rho = 1/2$ (because the sum of the peaks is equal to one due to the normalization of $P(V)$. Moreover, to produce $U_1 = 1/\gamma$ we must have a specific value W_2 such that $W_2\rho = 1/\gamma$, that is, $W_2 = 2/\gamma$, which is the same result obtained for $\mu = 0$, since it does not depends on μ (Fig. 12a). The point $W_2 = W_{\mathsf{B}} = 2/\gamma$ is indeed the bifurcation point for the marginally stable 2-cycle attractors, and the line $W_{\mathsf{B}}(\gamma)$ is the same as that obtained for $\mu = 0$.

Now lets consider the case of three peaks, where $U_1 < 1/\gamma$ and $U_2 \geq 1/\gamma$. The stationary equations for them are:

$$\rho = \eta_0 = \gamma U_1 \eta_1 + \eta_2 \,, \tag{47}$$

$$\eta_1 = \eta_0 \,, \tag{48}$$

$$\eta_2 = (1 - \gamma U_1)\,\eta_1 \,, \tag{49}$$

where the normalization condition $\sum_k \eta_k = 1$ holds. From the two first equations and $\eta_2 = 1 - \eta_0 - \eta_1 = 1 - 2\rho$ we get, remembering that $U_1 = W\rho$:

$$\gamma W \rho^2 - 3\rho + 1 = 0 \,, \tag{50}$$

with the solution,

$$\rho = \frac{3 - \sqrt{9 - 4\gamma W}}{2\gamma W} \,. \tag{51}$$

Notice that this solution is only valid when $P(V)$ has three peaks (and also with $W \leq 2/\gamma$). In the equality case, Eq. (51) gives $\rho = 1/2$ as expected.

The minimum value W_3 of W that produces three peaks is given by:

$$U_2 = 1/gamma \,, \tag{52}$$

$$\mu U_1 + W_3\rho = (\mu + 1)W_3\rho = 1/\gamma \,, \tag{53}$$

which gives

$$W_3 = \frac{1}{\gamma(\mu + 1)\rho} \,. \tag{54}$$

Inserting in Eq. (50) we get:

$$\rho = \frac{\mu + 1}{3\mu + 2} \,, \tag{55}$$

$$W_3 = \frac{3\mu + 2}{\gamma(\mu + 1)^2} \,. \tag{56}$$

As before, $\rho(W_3)$ does not depend on γ. As an example, if $\mu = 1/2$, we have that the minimum weight is $W_3 = \frac{14}{9\gamma} \approx \frac{1.5555}{\gamma}$ with $\rho(W_3) = 3/7 \approx 0.4285$ (Fig. 12b).

For an interval $W_4 < W < W_3$, $P(V)$ has four peaks and we follow the same calculation method. First we write the equations for the peaks:

$$\rho = \eta_0 = \gamma U_1 \eta_1 + \gamma U_2 \eta_2 + \eta_3 \,, \tag{57}$$

$$\eta_1 = \eta_0 \,, \tag{58}$$

$$\eta_2 = (1 - \gamma U_1)\,\eta_1 \,, \tag{59}$$

$$\eta_3 = (1 - \gamma U_2)\,\eta_2 \,, \tag{60}$$

with the normalization $\sum_{k=0}^{3}\eta_k = 1$. By using $\eta_3 = 1-\eta_0-\eta_1-\eta_2$ and $\eta_1 = \rho$ we obtain:

$$(\mu+1)(\gamma W)^2\rho^3 - (3+\mu)\gamma W\rho^2 + 4\rho - 1 = 0\,. \tag{61}$$

By solving for the roots of this third degree equation we obtain the solution for ρ (in the interval $[0,1]$). The point W_4 for the validity interval can be easily obtained by using the condition $U_3 = 1/\gamma$, leading to:

$$W_4 = \frac{1}{\gamma(\mu^2+\mu+1)\rho}\,. \tag{62}$$

Inserting in Eq. (61) gives, after some algebra:

$$\rho(W_4) = \frac{(\mu^2+\mu+1)^2}{4\mu^4+7\mu^3+8\mu^2+5\mu+2}\,. \tag{63}$$

For example, in the case $\mu = 1/2$, we have:

$$\rho(W_4) = \frac{49}{122} = 0.40163...\,, \tag{64}$$

$$W_4 = \frac{4}{7\gamma\rho} = \frac{488}{343\gamma} \approx \frac{1.4223}{\gamma} \tag{65}$$

(Fig. 12c). So, the solution from Eq. (61) with $\mu = 1/2, \gamma = 1$ is valid in the interval $W \in \left[1.4223\gamma; \frac{1.5555}{\gamma}\right]$.

Next we show that there is a regime where there is no peak above $V > 1/gamma$. This can be seem as follows:

$$U_k = \mu U_{k-1} + W\rho)\,, \tag{66}$$

$$U_0 = 0\,, \tag{67}$$

$$U_1 = W\rho\,, \tag{68}$$

$$U_2 = (1+\mu)W\rho\,, \tag{69}$$

$$U_3 = (1+\mu+\mu^2)W\rho\,, \tag{70}$$

$$U_k = \left(\sum_{j=0}^{k-1}\mu^j\right)W\rho\,, \tag{71}$$

$$U_\infty = \left(\sum_{j=0}^{\infty}\mu^j\right)W\rho = \left(\frac{1}{1-\mu}\right)W\rho\,. \tag{72}$$

So, imposing $U_\infty < 1/gamma$, we obtain that if $W\rho < (1-\mu)/\gamma$ there is no peaks above $V = 1$.

In this regime, we can calculate the position of the peaks as $U_k = W\rho\sum_{j=0}^{k-1}\mu^j$, which is a more direct form than the iterative one given by Eq. (46). By using all the previous analytic and numerical results (with maximal $k = 20$) we compare them with simulations with $N = 10000$ neurons (Fig. 8).

C. Monomial model with $\mu > 0$ and firing threshold V_T

For any r, a discontinuous phase transition occurs if we have a firing threshold $V_\mathsf{T} > 0$, as in the case with $\mu = 0$. We also have a bifurcation to 2-cycles at $W_\mathsf{B} = 2\left(\frac{1}{\gamma} + V_\mathsf{T}\right)$. A numerical phase diagram for $\gamma = 1, \mu = 1/2$ in the plane (W, V_T) (Fig. 13).

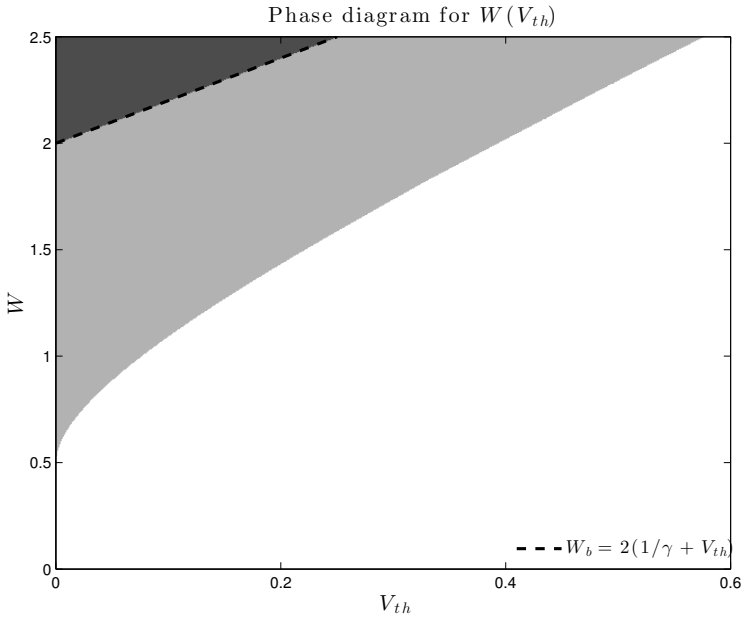

FIG. 13: Phase diagram for the linear monomial model with threshold V_T, $\gamma = 1$ and $\mu = 1/2$. We have a first order critical line $W_\mathsf{C}(V_\mathsf{T})$ determined numerically, and an analytic 2-cycle bifurcation line $W_\mathsf{B} = 2(1/\gamma + V_\mathsf{T})$.